Supplementary Information

Table S1. UV-Vis absorption characterization of TiO$_2$-aptamer complex at λ_{max} of 255 nm in HBB (pH 7.4).

S. No	Description	Absorbance
1.	Aptamer	0.139
2.	Aptamer-OTA	0.186
3.	Aptamer-OTA-TiO$_2$	0.195
4.	Aptamer-TiO$_2$	0.312

Selectivity of proposed TiO$_2$ based platform for OTA detection. The selectivity of proposed assay for OTA was also evaluated using three different concentration of Ochratoxin B (OTB). As can be clearly seen in Table S2, the obtained fluorescence response of OTB were accurate and less than 10% in comparison to OTA. Obtained results were attributed to the high selectivity of aptamer used for analysis of OTA.

Table S2. Specificity performance of TNPs assay for OTA detection.

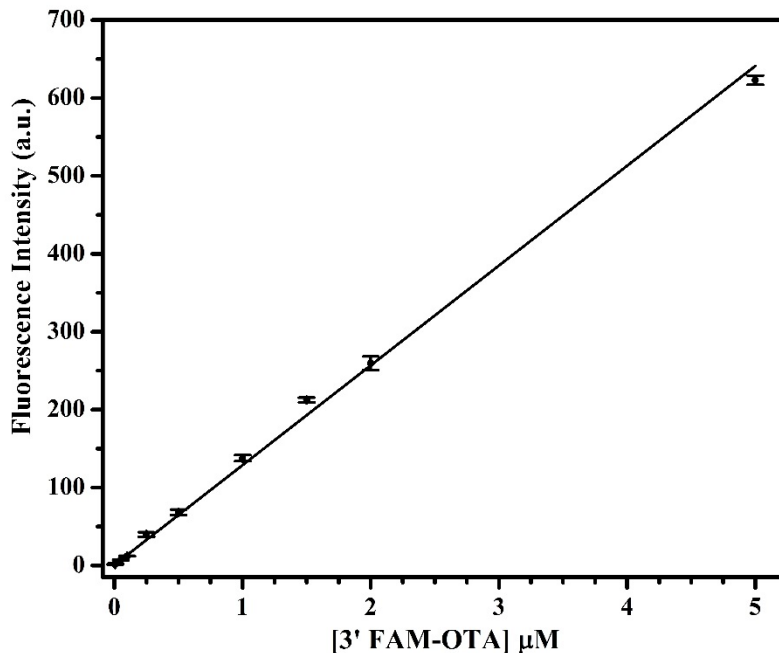| Concentration (µM)	OTA Recovered FL Intensity (%)		OTB Recovered FL Intensity (%)		% Response of OTB ($F_{OTB}/F_{OTA} \times 100$)
	Mean ± S.D. ($n = 3$)	% R.S.D.	Mean ± S.D. ($n = 3$)	% R.S.D.	
0.0031	7.11 ± 0.269	3.78	0.014 ± 0.0005	3.57	0.197
0.25	41.07 ± 2.199	5.35	0.961 ± 0.0515	5.36	2.339
10	92.22 ± 2.137	2.32	8.871 ± 0.2055	2.32	9.619

Figure S1. Optimization of FAM-labeled anti-OTA aptamer. The error bars were obtained from their parallel measurements.
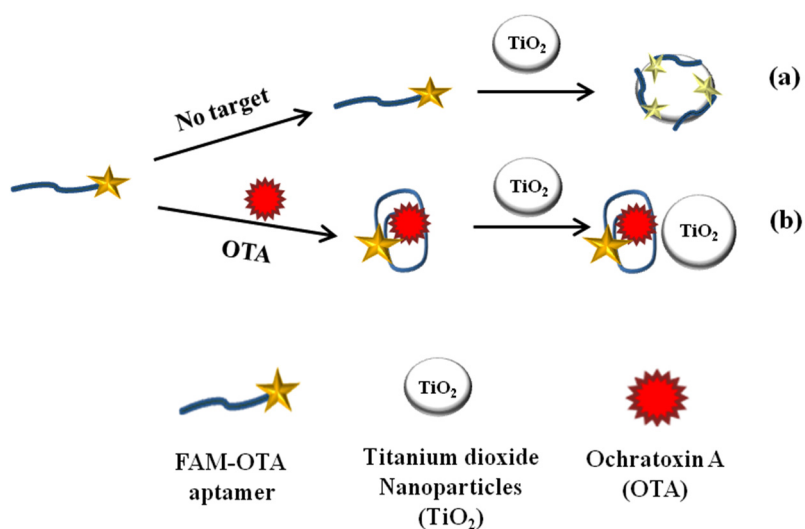
Figure S2. Schematic representation of TiO$_2$ quenching based aptamer assay for ochratoxin A (OTA). (**a**) Adsorption of FAM-labeled anti-OTA aptamer on TiO$_2$ surface causes fluorescence quenching; (**b**) In presence of OTA, the formation of anti-parallel G-quadruplex structure formation resist further adsorption and the fluorescence is recovered.